The Influence of Matrix Degradation and Functionality on Cell Survival and Morphogenesis in PEG-Based Hydrogels[a]

Asad Raza, Chien-Chi Lin*

Two norbornene-functionalized PEG macromers are synthesized to render hydrogels with different hydrolytic degradability. Dithiol-containing linkers such as dithiothreitol or biscysteine-containing peptides are used to control proteolytic degradability. The influence of thiol-ene gel degradability on cell survival and morphogenesis in 3D is assessed using hMSCs and pancreatic MIN6 β cells. The initial cell viability can be negatively affected in highly crosslinked thiol-ene hydrogels. When cells are encapsulated in thiol-ene gels lacking cell-adhesive motifs, their survival and proliferation are promoted in more hydrolytically labile hydrogels. The degree of 3D cell spreading in encapsulated hMSCs is enhanced when the matrices are immobilized with cell-adhesive motifs.

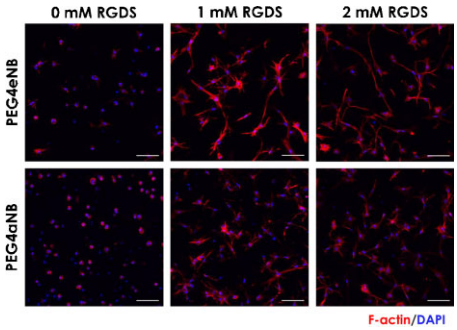

1. Introduction

Photopolymerized hydrogels prepared from poly(ethylene glycol) (PEG) have been used in a variety of tissue engineering applications[1–5] such as immunoisolation[6–8] and controlled cell differentiation.[9,10] PEG-based hydrogels are versatile biomaterials owing to their high permeability, tunable biophysical and biochemical properties, and excellent biocompatibility.[11–13] In particular, PEG-based hydrogels with tunable degradability offer user-controlled microenvironments for directing cell fate processes in 3D.[3,4,14–16] For example, PEG gels could be rendered hydrolytically degradable by copolymerizing PEG with poly(lactic acid) (PLA) or other ester-containing macromers.[17–20] The hydrolytic degradation of these chain-growth block co-polymer hydrogels could be predicted mathematically and these gels have been useful for cell culture in 3D.[17,20] Hydrolytically labile hydrogels could also be prepared via a step-growth photopolymerization mechanism. For instance, vinyl groups on PEG-tetra-acrylate or PEG-tetra-vinylsulfone macromers readily react with thiol groups on bi-functional linkers via nucleophilic Michael-type addition reactions, thus forming hydrogels with idealized network structure and predictable degradability.[11,21,22]

With respect to proteolytic degradation, Hubbell and colleagues pioneered the designs and applications of matrix metalloproteinase (MMP)-sensitive PEG-vinyl-sulfone hydrogels.[23,24] These gels were crosslinked by peptide substrates recognized by MMPs.[25] The gelation was achieved via a Michael-type conjugation reaction upon mixing macromer with thiol-containing peptide linkers. Alternatively, MMP-sensitive peptides could be modified with terminal PEG acrylates.[26,27] The gelation of these "acryl-PEG-peptide-PEG-acryl" macromers was achieved via the same chain-growth polymerization mechanism used to form PEGDA hydrogels. The inclusion of MMP-sensitive peptides allows cell-mediated local

A. Raza, Prof. C.-C. Lin
Department of Biomedical Engineering, Purdue School of Engineering and Technology, Indiana University-Purdue University at Indianapolis, Indianapolis IN 46202, USA
E-mail: lincc@iupui.edu

[a] **Supporting Information** is available from the Wiley Online Library or from the author

DOI: 10.1002/mabi.201300044

matrix remodeling, which is highly useful for tissue regeneration applications, such as accelerated bone healing.[23,24]

Initially introduced by Fairbanks and Anseth in 2009, PEG-peptide hydrogels fabricated from step-growth thiol-norbornene photo-click reactions have proven to be an attractive class of biomaterials.[28] Compared to chain-growth photopolymerization, step-growth thiol-ene photo-click reaction offers many beneficial properties, including mild and orthogonal reaction conditions, extremely rapid and highly tunable gelation kinetics, idealized network structures, as well as versatility in bioconjugation.[28] Although thiol-ene hydrogels are increasingly used as synthetic extracellular matrix (ECM) for 3D cell culture, studies correlating the material properties of thiol-ene hydrogel and its superior cytocompatibility remain limited and warrant further investigation.

Using the thiol-ene photopolymerization scheme, our laboratory has recently shown that radical-sensitive pancreatic β cells can be safely encapsulated with no significant cellular damage.[29] MIN6 β cells were able to proliferate in thiol-norbornene hydrogels even at a very low cell density (2×10^6 cells $\cdot$ mL^{-1}). In contrast, MIN6 cells encapsulated in chain-growth PEGDA hydrogels did not survive at low cell density.[29,30] When appropriate peptide substrates (e.g., CGGY↓C, where arrow indicates chymotrypsin cleavage site) were used as thiol-ene gel crosslinker, cell spheroids generated in situ were rapidly recovered via enzyme-mediated gel erosion.[29,31] In a separate study using experimental investigation and mathematical modeling, our laboratory has shown that thiol-ene gels formed by multi-arm PEG-ester-norbornene and dithiol-containing linkers were susceptible to base-catalyzed hydrolytic degradation.[32] Depending on the macromer formulations, the hydrolytic degradation rate of these thiol-ene hydrogels could be tuned from weeks to months.

Although our prior studies have investigated the mechanisms of hydrolytic degradation in thiol-ene hydrogels, a potential link between gel degradation and encapsulated cell fate has not been established. We hypothesized that hydrolytic degradation in thiol-ene hydrogels can promote cell survival, proliferation, and morphogenesis. To test this hypothesis, we synthesized two norbornene-functionalized PEG (PEG-NB) macromers: one through esterification between PEG-hydroxyl and norbornene acid, and another through amide bond formation between PEG-amine and norbornene acid. The use of these two macromers rendered hydrogels with different hydrolytic degradability. Gels prepared from PEG-amide-NB remained intact for the duration of study, whereas gels made by PEG-ester-NB degraded rapidly due to ester bond hydrolysis. In addition, the hydrolytic degradation rate of PEG-ester-NB hydrogels was controlled by tuning the macromer content or by changing the crosslinker chemistry (i.e., DTT or biscysteine containing peptide). In addition to gel degradability, we also examined the influence of thiol-ene reaction conditions on initial and long-term cell survival following photoencapsulation. Cells derived from mesenchymal tissues [e.g., human mesenchymal stem cells (hMSCs)] and epithelial tissues (e.g., pancreatic MIN6 β cells) were used in this study to establish the potential links between gel degradation and cell fate in 3D. In view of the importance of cell-mediated matrix remodeling on the survival and differentiation of hMSCs,[33] we incorporated an MMP sensitive peptide (KCGPQG↓IWGQCK) as the crosslinker in thiol-ene hydrogels to render the gels proteolytically degradable. Finally, a fibronectin-derived cell adhesive ligand, Arg-Gly-Asp-Ser or RGDS, was conjugated within the otherwise inert PEG-based hydrogels to illustrate the cooperative influence of gel degradation and cell/matrix interactions on cell survival and spreading.

2. Experimental Section

2.1. Materials

4-arm PEG-OH (20 kDa) and 4-arm PEG-NH_2 (20 kDa) were purchased from JenKem Technology (USA). Fmoc-amino acids, Fmoc-Rink-amide MBHA resin, and peptide synthesis reagents were purchased from Anaspec or Chempep. CellTiter Glo and AlamarBlue reagents were acquired from Promega and AbD Serotec, respectively. A live/dead staining kit for mammalian cells was purchased from Invitrogen. HPLC grade acetonitrile and water were acquired from Fisher Scientific and VWR International, respectively. All other chemicals were procured from Sigma-Aldrich unless noted otherwise.

2.2. PEG4eNB, PEG4aNB, and Photoinitiator Lithium Arylphosphinate (LAP) Synthesis

Degradable PEG-tetra-ester-norbornene (PEG4eNB) (Scheme 1a) was synthesized according to an established protocol with slight modifications.[28] Briefly, 4-arm PEG-OH was dried in a vacuum oven overnight and dissolved in anhydrous toluene. Toluene was evaporated using a rotary evaporator and the dried 4-arm PEG was dissolved in anhydrous dichloromethane (DCM). In a separate flask, 5-norbornene-2-carboxylic acid (5 equiv.) was reacted with *N,N'*-dicyclohexylcarbodiimide (DCC) (2.5 equiv.) in anhydrous DCM for at least 15 min at room temperature to form norbornene anhydride. The later was filtered through a fritted funnel and added drop-wise into a second flask (placed in an ice bath) containing dried 4-arm PEG-OH, 4-(dimethylamino)pyridine (DMAP) (0.5 equiv.), and pyridine (5 equiv.) in DCM. All of the reactions were performed under nitrogen. After overnight reaction, the product (PEG4eNB) was filtered, washed with 5 wt% sodium bicarbonate to remove unreacted norbornene acid and dried over sodium sulfate. The product was then filtered and precipitated in

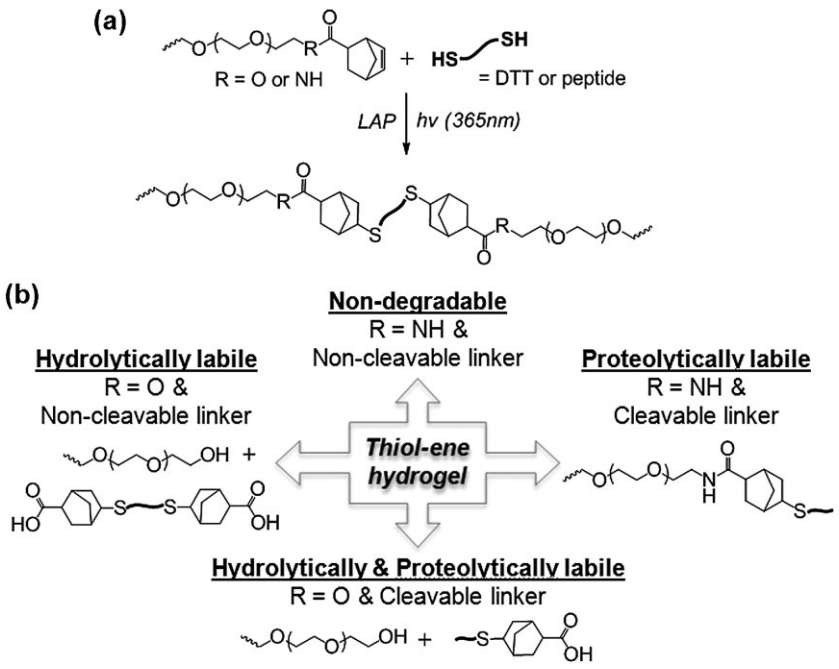

Scheme 1. Schematics of (a) thiol-ene photo-click reaction to form PEG-based hydrogels and (b) different modes of gel degradation. PEG-ester-norbornene (R = O) or PEG-amide-norbornene (R = NH) was used to construct gels with different hydrolytic degradability (only one arm of 4-arm PEG is shown). With a proper combination of macromer and crosslinker, the resulting hydrogels undergo different modes of degradation and produce different degradation products.

cold ethyl ether. The filtered product was re-dissolved in DCM and re-precipitated in cold ethyl ether to obtain the final product. PEG4eNB was dried overnight in vacuo and the degree of functionalization (>85%) was measured using proton NMR (Brucker 500).

Non-degradable PEG-tetra-amide-norbornene (PEG4aNB, Scheme 1a) was synthesized by reacting 4-arm PEG-NH_2 with norbornene carboxylic acid using HBTU/HOBT coupling chemistry. Briefly, 4-arm PEG-NH_2 was dried in a vacuum oven overnight and dissolved in anhydrous dimethylformamide (DMF). In a separate flask, norbornene carboxylic acid (5 equiv.) was activated by HBTU and HOBT (5.5 equiv.) in DMF for 3 min at room temperature. To the activated acid solution, DIEA (6 equiv.) was added and further reacted for 5 min under nitrogen. The mixture was then added drop wise to the flask containing 4-arm PEG-NH_2 and allowed to react overnight. PEG4aNB was obtained by precipitation in cold ether and further purified using protocol similar to PEG4eNB purification procedure. The degree of functionalization (>85%) was measured using proton NMR.

The photoinitiator LAP was synthesized according to a published protocol without modification.[34]

2.3. Peptide Synthesis and Purification

All of the peptides were synthesized using standard solid phase peptide synthesis (SPPS) chemistry in a microwave peptide synthesizer (CEM Discover SPS) following the manufacturer's recommended synthesis procedures. The peptides were also cleaved in the microwave peptide synthesizer (38 °C, 20 W, 30 min) using a cleavage cocktail containing 95% trifluoroacetic acid (TFA), 2.5% water, and 2.5% triisopropylsilane (TIS) in the presence of 5% w/v phenol. Crude peptides were precipitated in cold ethyl ether, dried overnight in a desiccator, purified using HPLC (Perkin–Elmer Flexar System), and characterized by mass spectrometry (Agilent Technologies). Purified peptides were lyophilized and stored in −20 °C. The concentration of thiol groups on purified cysteine-containing peptides was quantified using Ellman's reagent (PIERCE).

2.4. Hydrogel Fabrication and Characterization

Thiol-norbornene hydrogels formed by step-growth photopolymerization were fabricated using PEG4eNB or PEG4aNB (20 kDa) and di-thiol crosslinkers, such as DTT or bis-cysteine containing peptide CGGYC[29] or KCGPQGIWGQCK.[35,36] Radical-mediated thiol-norbornene photopolymerization was initiated using 10^{-3} M LAP dissolved in phosphate-buffered saline (PBS) under long-wave UV light exposure (365 nm, 5 mW · cm^{-2}) for 3 min (Scheme 1a). For all of the hydrogel formulations, a stoichiometric ratio between thiol and norbornene groups was maintained. Gels (50 μL) were formed in 1 mL disposable syringes with cut-open tips.

Following thiol-norbornene photopolymerization, hydrogels were incubated at 37 °C in double distilled (dd) H_2O on an orbital shaker for 24 h to remove all unreacted macromers. The gels were then dried in vacuum for 24 h to obtain dried gel weight (W_{dry}). Dried gels were then incubated in PBS at 37 °C on an orbital shaker. At predetermined time points (i.e., 2, 4, 7, and 10 d), the hydrogel swollen weights ($W_{swollen}$) were measured gravimetrically and were used to calculate the mass swelling ratio (q), which is defined as: $W_{swollen}/W_{dry}$. The mass swelling ratios were used to calculate hydrogel mesh size based on the Flory–Rehner theory as described elsewhere.[3]

2.5. Cell Culture and Encapsulation

Murine pancreatic β cells (MIN6) were maintained in high glucose Dulbecco's modified Eagle medium (DMEM) (HyClone) containing 10% fetal bovine serum (Gibco), 1× antibiotic-antimycotic (Invitrogen, 100 U · mL^{-1} penicillin, 100 μg · mL^{-1} streptomycin, and 250 ng · mL^{-1} fungizone), and 5×10^{-5} M β-mercaptoethanol. hMSCs were isolated from human bone marrow (Lonza) and maintained in low glucose DMEM (HyClone) containing 10% fetal bovine serum (Gibco), 1× Antibiotic-Antimycotic (Invitrogen, 100 U · mL^{-1} penicillin, 100 μg · mL^{-1} streptomycin, and 250 ng · mL^{-1} Fungizone), and 1 ng · mL^{-1} recombinant human

*b*FGF (PeproTech). Cells were cultured in tissue culture plastic kept at 37 °C and 5% CO_2 and the culture medium was changed every 2–3 d. hMSCs were used in passages 2–4.

Cell encapsulation was performed using a procedure similar to the gel fabrication method described earlier. Briefly, MIN6 β-cells or hMSCs (at a cell density of 2×10^6 cells $\cdot$ mL^{-1}[29] or 5×10^6 cells $\cdot$ mL^{-1},[33] respectively) were suspended in pre-polymer solutions containing PEG macromer, crosslinker, CRGDS (for some experimental groups) and photoinitiator, and exposed to UV light (365 nm, 5 mW $\cdot$ cm^{-2}) for 2 min. A shorter (2-min) photopolymerization time was used in cell encapsulation to avoid unnecessary UV exposure to the cells. Our previous in situ rheometry result showed that complete thiol-ene gelation was achieved in 2 min.[32] Cell-laden hydrogels (25 μL) were maintained in identical cell culture conditions as described earlier on an orbital shaker.

2.6. Encapsulated Cell Viability Assays

To measure initial cell viability in hydrogels, cell-laden hydrogels were incubated in buffers containing 75 μL of HBSS (for MIN6 β cells) or DPBS (for hMSCs) and 75 μL of CellTiter Glo reagent following photopolymerization. After 1 h of incubation, intracellular ATP concentration was quantified by measuring sample luminescence using a microplate reader (Synergy HT, BioTek Instruments). Intracellular ATP concentrations were interpolated from a series of known ATP monohydrate concentrations.

Qualitative cell viability following photoencapsulation was determined using live/dead staining and confocal imaging. Cell-laden hydrogels were incubated in live/dead staining solution for 1 h at room temperature with gentle shaking. Confocal images of the stained samples were obtained using Olympus Fluoview FV100 Laser Scanning Biological Microscope (IUPUI Nanoscale Imaging Center). *z*-Stack images (100 μm thick, 10 μm per slice) from three samples and at least four random fields were acquired for every experimental condition. A total of at least 12 *z*-stack images were utilized for counting live (staining green) and dead (staining red) cells for all the experimental groups. Cell viability was quantified by calculating percentage of live cells relative to total number of cells.

To monitor long term cell viability and proliferation, cell-laden hydrogels were incubated in 500 μL of 10% AlamarBlue reagent in cell culture medium for 16 h (for MIN6 β cells) or 14 h (for hMSCs). Following incubation, 200 μL of the media was transferred to a 96-well plate and fluorescence generated due to non-specific cellular metabolic activity was measured using a microplate reader (excitation: 560 nm, emission: 590 nm). Live/dead staining was also used to visualize cell morphology within hydrogels at day 10. All of the live/dead images were analyzed using Olympus Fluoview and NIH ImageJ software.

2.7. Analysis of Cell Morphology and F-Actin Staining

z-Stack confocal images (100 μm thick) of live/dead staining were used to visualize hMSCs spreading and MIN6 cell spheroid size at day-10 post-encapsulation. Images from four samples and at least three random fields per sample were acquired for analysis using Olympus Fluoview software and results were confirmed with NIH ImageJ. Cell length was defined as the longest end-to-end distance of a straight line connecting the two end points on a cell. MIN6 β cell spheroid sizes were acquired by measuring the spheroid diameter in both the *x* and *y* directions. The average of the two diameters was reported as cell spheroid diameter. To visualize F-actin expression in hMSCs, cell-laden hydrogels were fixed in 4% paraformaldehyde at room temperature for 45 min with gentle shaking. Samples were then washed with PBS twice (5 min each) and the cells were permeabilized using 0.5% Triton X-100 in PBS at room temperature for 45 min with gentle shaking. Following permeabilization, samples were washed with PBS twice and incubated in blocking buffer [5% bovine serum albumin (BSA), 5% fetal calf serum, and 5% poly(vinyl pyrrolidone) (PVP) in PBS] overnight at 4 °C. Samples were then washed and incubated in rhodamine-labeled phalloidin overnight at 4 °C, followed by washing in buffer containing 0.5% Tween-20 and 5% BSA overnight at 4 °C. Cell nuclei were counter-stained with DAPI for 1 h and washed with PBS. *z*-Stack images (100 μm thick) were taken using Olympus Fluoview FV100 confocal microscope.

2.8. Statistical Analysis

All of the experiments were conducted independently for three times and the results were presented as mean ± standard deviation (SD). Statistical significance between selected groups was determined using Student's *t*-test. Difference between conditions was considered statistically significant when $p < 0.05$.

3. Results and Discussion

3.1. Effect of Macromer Composition on Hydrolytic Degradation of Thiol-Ene Hydrogels

Depending on the macromer and crosslinker chemistry, thiol-ene hydrogels can be rendered completely non-degradable, degradable only by hydrolysis *or* proteolysis, or degradable by hydrolysis and proteolysis (Scheme 1b). We hypothesized that hydrogel degradability plays an important role in maintaining long-term cell survival in thiol-norbornene hydrogels. We synthesized two PEG-norbornene macromers with different degradability: one with hydrolytically stable amide bond (i.e., PEG4aNB) and one with hydrolytically labile ester bond (i.e., PEG4eNB) connecting the PEG backbone and the norbornene group. Using these two macromers with different dithiol-containing linkers (e.g., DTT, CGGYC, or KCGPQGIWGQCK), we performed gel swelling/degradation studies for a period of 10 d (Figure 1). Hydrogel swelling profiles diverged as time due to the difference in macromer degradability and crosslinker type. While PEG4eNB hydrogels degraded in buffer solution (pH = 7.4) gradually, hydrogels prepared from amide-linked PEG4aNB macromer did not degrade over a period of 10 d, regardless of the crosslinkers used (Figure 1). The hydrolytic degradation mechanism of PEG4eNB-based hydrogels has been studied experimentally and verified by a model prediction.[32] Even with the use

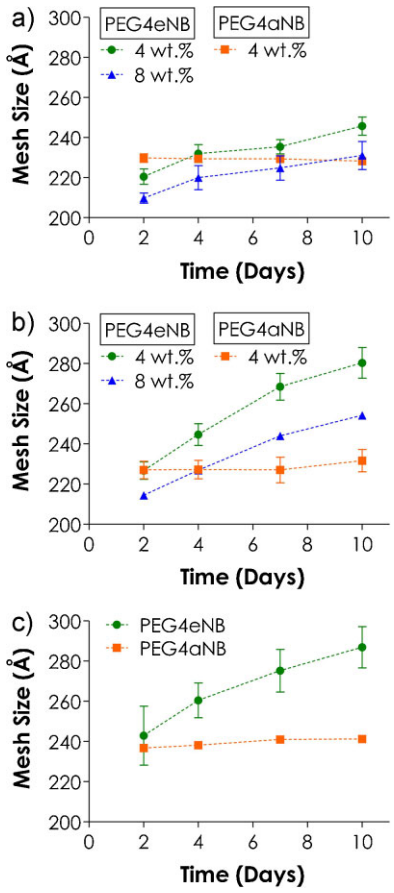

Figure 1. Effect of macromer compositions on mesh size (i.e., degradation) of thiol-ene hydrogels. PEG4eNB or PEG4aNB was used as macromer. Crosslinkers used were: (a) DTT, (b) CGGYC, and (c) KCGPQGIWGQCK. 4 wt% PEG macromer was used in (c) ($N = 4$, mean ± SD).

of hydrolytically labile PEG4eNB macromer, the degradation rate of hydrogels varied. For example, PEG4eNB hydrogels crosslinked by peptide linker (i.e., CGGYC in Figure 1b or KCGPQGIWGQCK in Figure 1c) degraded faster than DTT crosslinked gels (Figure 1a). While these two peptides contained no hydrolytically labile motifs in their backbones, the presence of different amino acid side groups in the peptide crosslinkers likely altered water accessibility to the crosslinks and changed the hydrolysis rate of ester bonds on PEG4eNB. These results were consistent with our earlier report regarding the degradation mechanism of PEG-norbornene hydrogels.[32]

In addition to the crosslinker chemistry, hydrogel degradability was also affected by macromer concentration. Hydrogels formed by a higher macromer content (e.g., 8 wt%) had lower initial mesh sizes regardless of the crosslinker used (Figure 1a, b). This phenomenon was attributed to a higher network crosslinking efficiency at higher macromer concentrations.[32] Furthermore, the swelling and mesh size of hydrogels crosslinked by both macromer contents (i.e., 4 and 8 wt%) when incubated in a buffer solution increased steadily over a period of 10 d (Figure 1a, b). It is worth noting that the swelling of PEG hydrogels is tightly coupled to the gel mesh size and mechanical properties due to a bulk degradation mechanism in these gels.[37] It has been shown that the mechanical properties of highly swollen PEG hydrogels are correlated inversely to the swelling behaviors.[32,37,38]

To evaluate the influence of cellular activity on hydrogel degradation, we encapsulated hMSCs in PEG4aNB or PEG4eNB hydrogels crosslinked by MMP-sensitive peptide linker with or without immobilized RGD motif (1 or 2×10^{-3} M). Similar to data shown in Figure 1c, gel degradation was more pronounced in PEG4eNB hydrogels than in PEG4aNB hydrogels (data not shown). One would anticipate this level of degradation to play a significant role in cell fate determination in hydrogels. Prior reports pertinent to thiol-norbornene hydrogels, however, did not evaluate the effect of this critical factor on long-term cell viability and morphogenesis.

3.2. Effect of Macromer Content on Cell Viability Following In Situ Photoencapsulation

To understand the effect of thiol-norbornene hydrogel properties on cell survival and morphogenesis, it is important to examine the initial cell viability following in situ gelation and encapsulation. Thus, immediately following photo-encapsulation we assessed the viability of the encapsulated cells qualitatively using live/dead staining and quantitatively with CellTiter Glo reagent. We found that increasing macromer concentration from 4 to 8 wt% decreased viability of encapsulated hMSCs from 87 ± 2% to 74 ± 3% in CGGYC crosslinked PEG4eNB hydrogels, and from 82 ± 1% to 70 ± 4% in DTT crosslinked PEG4eNB hydrogels (Figure 2a). The effect of macromer concentration and crosslinker type on initial cell viability was also assessed quantitatively by intracellular ATP measurements (Figure 2b). These ATP assays were conducted one-hour post-encapsulation and the results correlated directly to the number of metabolically active cells following photo-encapsulation. Not surprisingly, these quantitative results agree with the qualitative images shown in Figure 2a, confirming the negative influence of high functional group concentrations on cell survival during and following photoencapsulation. Similar reduction in initial cell viability at higher macromer content was also found in encapsulated MIN6 β-cells (Figure S1 in the Supporting Information).

The decreased initial cell viability at higher macromer concentrations could be attributed to: i) higher amount

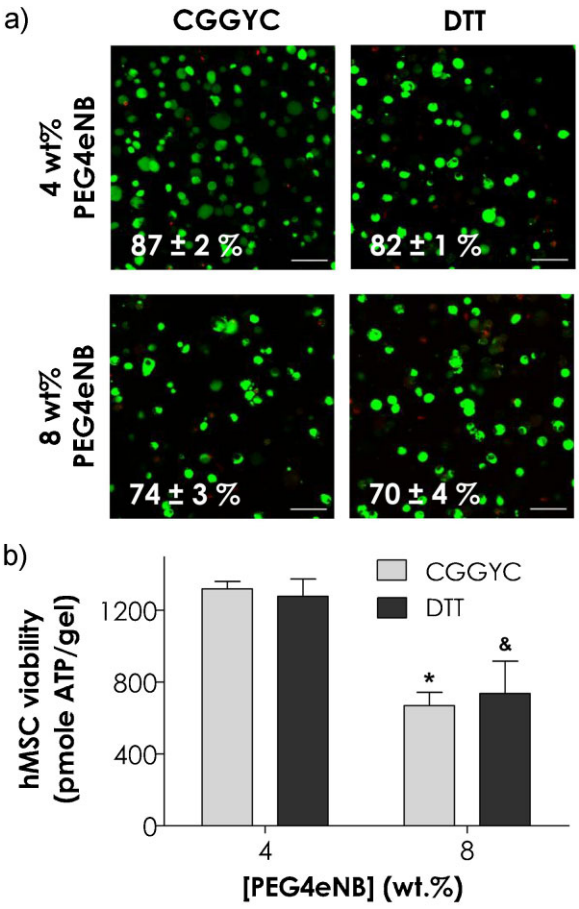

Figure 2. Effect of hydrogel formulation on initial viability of hMSCs encapsulated in PEG4eNB hydrogels crosslinked by different linkers indicated. (a) Cell-laden hydrogels were stained with a live/dead staining kit and imaged by confocal microscopy. The numbers shown in the representative confocal *z*-stack images are the percentages of live cells over the total cell count (Scale: 100 μm; $N = 4$, mean ± SD). (b) Intracellular ATP concentrations were determined by CellTiter Glo reagent 1 h post-encapsulation. ($N = 4$, mean ± SD). The asterisk and ampersand represent $p < 0.05$ within the respective group (i.e., compared to 4 wt% gels).

of radical species generated on the functional groups during network crosslinking and ii) higher degree of crosslinking at higher macromer concentrations. It has been shown that cells are sensitive to radical species generated during photopolymerization reaction.[29] When macromer concentration was raised from 4 to 8 wt%, the total functionality (i.e., thiol and norbornene groups) in the pre-polymer solution was increased by 100% from 1.6 to 3.2×10^{-2} M. This drastic increase in macromer functionality resulted in higher radical concentration and higher extent of thiol-norbornene click reaction,[32,39] both of which might contribute to decreased initial cell viability. Additionally, increased macromer content in the pre-polymer solution led to a higher network crosslinking density,[32,40,41] which could cause negative influence on initial cell survival. For all of the macromer concentrations used, however, we did not observe significant differences in cell viability between gels formed by different macromer type (i.e., PEG4eNB or PEG4aNB) or crosslinkers (i.e., DTT or CGGYC). This was due to a similar degree of crosslinking reactions at the same functional group concentration.

While the initial viability decreased with increasing macromer concentration, most of the cells survived the photo-encapsulation process (≈70–90%), even at low cell densities. As a comparison, previous studies showed that only about 40% of the encapsulated β-cells survived following photoencapsulation in chain-growth PEGDA hydrogels at a cell density of 6.7×10^6 cells · mL^{-1} and essentially no cell survived when the cell density was lower than 5×10^6 cells · mL^{-1}.[30] Another study showed that, even at an extremely high cell density of 25×10^6 cells · mL^{-1}, only about 77% of the encapsulated hMSCs survived in UV-initiated chain-growth PEGDA hydrogels.[42] These results suggested that cell density, crosslinking conditions (e.g., identity of macromers and initiators), as well as polymerization mechanisms collectively affect initial cell viability in PEG-based hydrogels.

3.3. Effect of Hydrolytic Gel Degradation on Cell Viability

Previously we have shown that PEG hydrogels formed by thiol-norbornene photo-click reactions supported the formation of MIN6 β-cells spheroids in 3D.[29] Using thiol-norbornene gels with identical macromer chemistry, Anderson et al. showed that proteolytic degradation was beneficial in the survival and differentiation of hMSCs.[33] These reports did not, however, examine the influence of hydrolytic degradation in thiol-norbornene hydrogels on the observed cell behaviors. We hypothesized that hydrolytic degradation in the ester-containing PEG4eNB macromer will have beneficial effects on cell viability for both mesenchymal (e.g., hMSCs) and epithelial (e.g., MIN6) cell types. To test this hypothesis, we first assessed the viability of encapsulated hMSCs and MIN6 β cells qualitatively using live/dead staining (Supporting Information, Figure S2 for hMSCs and Figure S3 for MIN6) and quantitatively using AlamarBlue reagent (Figure 3 for hMSCs and Supporting Information, Figure S4, for MIN6). The majority of cells survived in all of the gel formulations tested over a period of 10 d for both hMSCs and MIN6. While hMSCs retained their round and dispersed morphology (Supporting Information, Figure S2) without the presence of ECM-mimetic motif (e.g., RGD peptide), MIN6 β cells formed spherical aggregates (Supporting Information, Figure S3) in all of the hydrogels after 10 d culture. Quantitative viability assay showed that

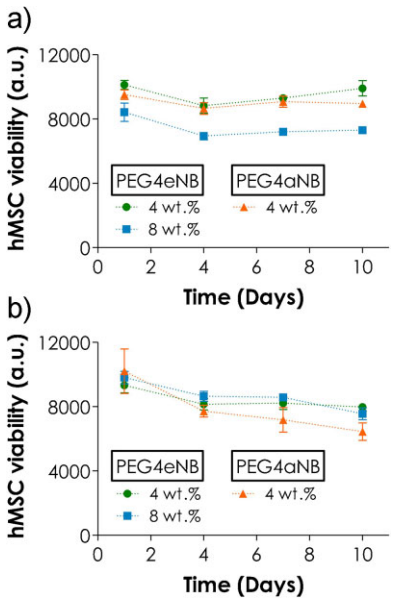

Figure 3. Effect of hydrogel formulation on sustaining hMSCs survival in: (a) CGGYC or (b) DTT crosslinked hydrogels. Cell viability as time was determined quantitatively by AlamarBlue reagent ($N = 3$, mean $\pm$ SD).

hMSCs encapsulated in degradable PEG4eNB gels crosslinked by CGGYC roughly maintained their viability throughout the 10 d culture period (Figure 3a). Unfortunately, cell viability dropped almost monotonically as time in gels that degraded slowly (higher PEG wt% or DTT-crosslinked) or lacking significant hydrolytic degradation (with PEG4aNB) (Figure 3b). On the other hand, PEG4eNB hydrogels crosslinked by CGGYC peptide supported the formation of larger MIN6 spheroids compared to using DTT as crosslinker (45 ± 1 vs. 39 ± 1 μm, Figure S3c, S3d in the Supporting Information). Moreover, MIN6 β cell spheroids formed in non-degradable PEG4aNB hydrogels, regardless of the crosslinkers used, appeared much smaller (≈21 μm) compared to the hydrolytically degradable gels (Figure S3 in the Supporting Information). Quantitative cell proliferation assay agrees with the qualitative live/dead staining (Figure S4 in the Supporting Information). The promoting effect on cell proliferation due to gel degradation was more prominent in proliferative MIN6 cells when comparing the two crosslinkers (CGGYC in Figure S4a and DTT in Figure S4b in the Supporting Information). For example, the degree of MIN6 β cells proliferation in 4 wt% CGGYC-crosslinked hydrogels was roughly 2.5-fold higher than that in DTT-crosslinked gels.

As noted earlier, encapsulated hMSCs retained round and single cell morphology in the gels without cell adhesive ligands (Figure S2 in the Supporting Information). The morphological differences in epithelial and mesenchymal cells in 3D have been reported in other publications.[33,43,44] However, the potential connections between hydrolytic degradation in thiol-ene hydrogels and the survival and morphological changes of hMSCs in 3D have not been established. As shown in Figure 1, hydrolytically labile thiol-ene hydrogels used in this contribution had only 10–30% increase in the calculated network mesh size. It is worth noting, however, that the determination of hydrogel mesh size was based on bulk hydrogel swelling. The rate of local ester bond hydrolysis might be accelerated due to the secretion of esterase by some cells. Techniques such as particle-tracking microrheology can be used in the future to correlate local changes in cell-laden gel degradation to bulk gel properties.[45,46] While the changes in cell fate determination observed in this study cannot be exclusively attributed to bulk gel degradation, its positive correlation to cell viability/proliferation suggests an important role of hydrolytic matrix degradation. The changes in other material properties, such as gel modulus or swelling, were consequences of gel degradation and should be considered as an integral part that collectively affected cell behaviors in 3D. Mechanistic understanding of cell behavioral changes due to the influence of these factors will benefit from advanced techniques capable of isolating the influence of individual hydrogel parameter related to degradation.

3.4. Effect of Cell-Adhesive Motif and Hydrolytic Gel Degradation on hMSC Viability

It should be noted that results shown in the previous sections were obtained from PEG-based hydrogels without the presence of cell-adhesive moieties, which have proven beneficial in supporting cell survival in 3D.[1,47,48] We were interested in illustrating the potential synergistic influence of gel hydrolytic degradation and cell-adhesive motifs, such as fibronectin-derived RGDS, on cell survival and morphogenesis. Toward this end, we monitored the viability of hMSCs encapsulated in CGGYC peptide crosslinked gels incorporated with 0, 1, and 2×10^{-3} M of CRGDS (Figure 4). Interestingly, the influence of cell adhesive RGDS motif on cell survival was very marginal in hMSCs encapsulated in hydrolytically labile PEG4eNB hydrogels (Figure 4a). However, the promoting effect of RGDS peptide in cell viability was higher in non-hydrolytically labile PEG4aNB hydrogels (Figure 4b). Note that in both cases, cell-secreted proteases have minimal effect on proteolytic degradation of the network due to the use of CGGYC peptide linker. Hence, the major difference between these two gel formulations (i.e., PEG4eNB and PEG4aNB) was the hydrolytic degradability of PEG macromer. We believe that the encapsulated cells experienced more strain imposed by the crosslinked polymer mesh in non-hydrolytically labile PEG4aNB

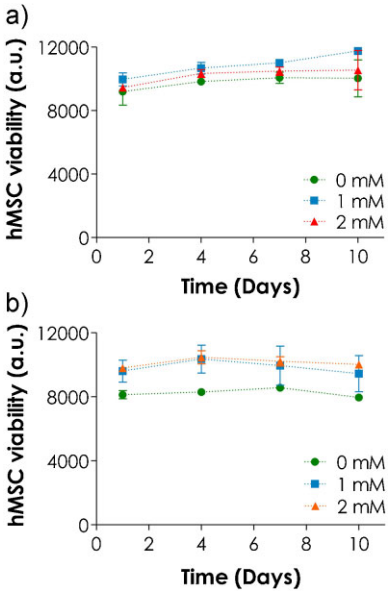

Figure 4. Effect of cell/matrix interaction on sustaining survival of hMSCs in: (a) CGGYC or (b) DTT crosslinked hydrogels. Cell viability as time was determined quantitatively by AlamarBlue reagent. Cells were encapsulated in hydrogels immobilized CRGDS with 0, 1, or 2×10^{-3} M ($N = 3$, mean ± SD).

hydrogels. Consequently, the inclusion of RGDS ligand enhanced cell viability by providing critical cell/matrix interactions that were otherwise lacking.

Murphy and colleagues have previously reported enhanced viability of hMSCs encapsulated in hydrolytically degradable Michael-type PEGDA-DTT hydrogels.[49–51] While our results reaffirm the effect of RGDS ligand on improving hMSC viability in PEG-based hydrogels, the use of thiol-ene hydrogels with various degrees of hydrolytic degradability (i.e., PEG4eNB or PEG4aNB macromer) further highlights the critical role of hydrolytic degradation in relation to cell/matrix interactions.

3.5. Effect of Hydrolytic Gel Degradation, Cell-Mediated Matrix Remodeling, and Cell/Matrix Interaction on hMSC Viability and Morphology

Thiol-ene hydrogels can be designed to undergo cell-mediated local matrix remodeling by incorporating protease (e.g., MMPs) sensitive peptides as gel crosslinkers.[28] Selective cleavage of matrix locally by cell-secreted proteases alters the extent of cell/matrix interactions, which impact cell fate determination.[33,52] For example, Anderson et al. showed that the degree of proteolytic degradation in thiol-ene hydrogels affected the survival, proliferation, and differentiation of hMSCs.[33] Given the profound impact of gel hydrolytic degradation on cell survival as shown in Figure 2–4, we reasoned that these two forms of gel degradation (i.e., proteolytic and hydrolytic) might collaboratively affect hMSCs viability and morphology under the influence of cell/matrix interactions provided by immobilized integrin ligand RGDS.

We encapsulated hMSCs in PEG4eNB or PEG4aNB hydrogels crosslinked by an MMP-sensitive peptide linker (i.e., KCGPQG↓IWGQCK) incorporated with 0, 1, and 2×10^{-3} M of CRGDS. Cell morphology was visualized using live/dead staining and confocal imaging after 10 d culture. In the absence of RGDS ligand (Figure 5a, left column), cells retained round and single cell morphology even with the use of MMP-sensitive peptides as gel crosslinker. Without RGDS ligand, almost no difference was found in cell morphology between hydrolytically

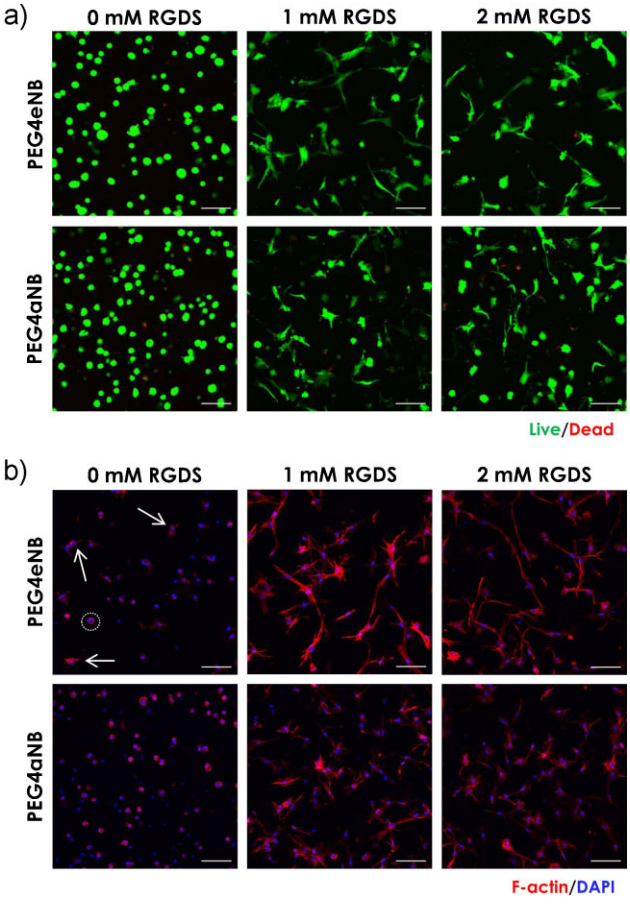

Figure 5. Effect of hydrogel degradability and cell/matrix interaction on hMSC morphology 10 d post-encapsulation. Cell-laden hydrogels were stained with (a) Live/dead staining kit or (b) Rhodamine-labeled phalloidin for F-actin. Cell nuclei were counter stained with DAPI. Arrows indicate cells with protrusions while dotted circle indicates cells with concentric F-actin expression. Cells were encapsulated in 4 wt% PEG4eNB or PEG4aNB hydrogels crosslinked by MMP-sensitive peptide linker (KCGPQGIWGQCK) and immobilized with 0, 1, or 2×10^{-3} M of CRGDS. Stained cell-laden hydrogels were imaged by confocal microscope (scale: 100 μm).

labile PEG4eNB and hydrolytically stable PEG4aNB hydrogels. When RGDS ligand was incorporated, hMSCs exhibited long cellular processes in both gel systems. However, the amount of cells exhibiting long processes due to enhanced local matrix degradation was higher in hydrolytically labile PEG4eNB-based hydrogels than in hydrolytically stable PEG4aNB-based gels (Figure 5a, middle and right columns). We further analyzed the degree of cell spreading by measuring cell length from the live/dead staining images (Figure S5a in the Supporting Information). Over 90% of the cells in the "dual-mode" (i.e., hydrolytic and proteolytic) degradable PEG4eNB hydrogels had cellular processes longer than 30 μm and the average cell length (longest end-to-end distance) was over 80 μm (Figure S5b in the Supporting Information). On the other hand, only ≈50% of the cells had processes longer than 30 μm in the "single mode" (i.e., only proteolytic) degradable PEG4aNB hydrogels and the average cell length was only about 47 μm. Additionally, in the dual-mode degradable hydrogels, increasing RGDS ligand concentration from 1 to 2×10^{-3} M did not yield further increase in the percentage of cells exhibiting long processes or the average cell length. This was likely due to saturation of integrin/RGD interactions in the highly degradable microenvironment. However, as RGDS concentration was increased from 1 to 2×10^{-3} M, slightly but not statistically significant increases in cell spreading were observed in the single mode degradable PEG4aNB hydrogels. Further, the differences in cell spreading decreased as RGDS ligand concentration was raised from 1 to 2×10^{-3} M when comparing the spreading of hMSCs in PEG4eNB and in PEG4aNB hydrogels.

Regardless of the crosslinker used, one can see that the morphology of live/dead stained hMSCs appeared similar (i.e., round, single cell) in gels without cell-adhesive ligand (comparing Figure 5a left column to Figure S2 in the Supporting Information). To further evaluate the influence of hydrolytic gel degradation on cell phenotype in relation to cell adhesiveness, we conducted immunostaining for F-actin and counter-stained cell nuclei with DAPI (Figure 5b). While the F-actin staining results were in line with the live/dead staining images shown in Figure 5a, the critical effect of hydrolytic degradation was more profound in the F-actin staining images. For example, in the absence of RGDS ligand (Figure 5b, left column), the expression of F-actin appeared to be less condensed in most cells encapsulated in the dual-mode (i.e., hydrolytic and proteolytic) degradable PEG4eNB hydrogels. It can be seen that some cells in the dual-mode degradable PEG4eNB hydrogels showed short protrusions (white arrows) and very few cells exhibited concentric F-actin expression (dotted circle). When the cells were encapsulated in the single-mode (i.e., proteolytic only) degradable PEG4aNB hydrogels, most of the cells expressed F-actin concentric to cell nuclei with no protrusion. While these gels were all crosslinked by the same MMP-sensitive peptide linker, hMSCs failed to show extensive spreading due to the lack of integrin-mediated signaling. However, hMSCs encapsulated in the dual-mode degradable PEG4eNB hydrogels showed slightly higher degree of local matrix remodeling. In the presence of 1 or 2×10^{-3} M RGDS (Figure 5b, middle and right columns), most of the cells exhibited multiple long processes in both the dual-mode degradable PEG4eNB and single-mode degradable PEG4aNB hydrogels. This phenomenon was even more apparent in the dual-mode degradable PEG4eNB hydrogels. These results are in consistent to the results shown by Anderson et al., where hMSCs exhibited extensive cellular processes only when they were encapsulated in an MMP-sensitive microenvironment and in the presence of RGDS motif.[33]

Using AlamarBlue reagent, we further assessed hMSCs viability in MMP-sensitive peptide crosslinked hydrogels in relation to integrin ligand RGDS (Figure 6). In general, hMSCs encapsulated in the dual-mode degradable PEG4eNB hydrogels had higher viability compared to the use of gels with only proteolytic degradability (i.e., PEG4aNB gels). In the absence of RGDS ligand, however, viability only increased slightly over the course of 10 d culture (Figure 6a). On the contrary, hMSCs encapsulated in RGDS-immobilized PEG4eNB or PEG4aNB hydrogels showed increased viability as time (Figure 6b,c). Interestingly, the difference in cell viability between PEG4eNB and PEG4aNB hydrogels was higher in gels without (Figure 6a) or with 1×10^{-3} M of RGDS (Figure 6b). The difference in cell viability in these two types of gels (PEG4eNB and PEG4aNB) diminished when the concentration of immobilized RGDS was raised to 2×10^{-3} M (Figure 6c). This was similar to the trend observed in the 3D spreading of hMSCs as shown in Figure 5. Similar to the cell viability data shown in Figure 4, enhanced hydrolytic gel degradation likely compensates the adverse effect elicited by the lack of cell/matrix interaction.

Collectively, these results suggest that hydrolytic degradation, proteolytic degradation, and cell/matrix interactions work together in enhancing the viability and spreading of hMSCs encapsulated in PEG-based hydrogels. The hydrolytic degradation of PEG4eNB hydrogels likely enhanced cell/matrix interactions that led to higher degree of cell spreading. This phenomenon reveals that hydrolytic gel degradation could be exploited to achieve a similar level of intracellular signaling at a lower concentration of bioactive motif. While not the focus of the current study, these factors are expected to impact how hMSCs differentiate in an artificial ECM with well-controlled and well-orchestrated matrix properties.

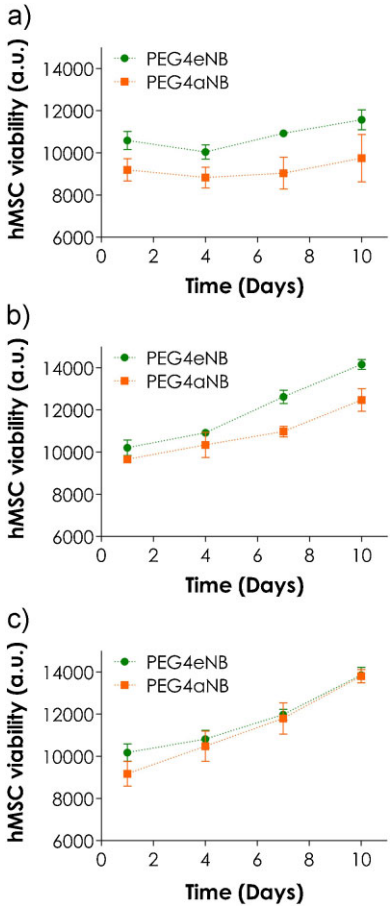

Figure 6. Effect of hydrogel degradability and cell/matrix interaction on sustaining cell survival and proliferation. hMSCs were encapsulated in 4 wt% PEG4eNB or PEG4aNB hydrogels crosslinked by MMP-sensitive linker (KCGPQGIWGQCK) and immobilized with (a) 0×10^{-3} M, (b) 1×10^{-3} M, or (c) 2×10^{-3} M of CRGDS. Viability as time was determined by AlamarBlue reagent ($N = 3$; mean ± SD).

4. Conclusion

We have shown that thiol-norbornene hydrogels could be designed to remain stable, or be tuned to degrade hydrolytically and/or proteolytically. Compared to single mode degradable gels, dual-mode degradable thiol-norbornene hydrogels provided a more cytocompatible environment for promoting cell survival, proliferation, and morphogenesis in 3D. Lower macromer contents reduced initial cell damage during in situ photo-encapsulation due to lower radical concentration, lower degree of crosslinking reaction, and decreased network crosslinking density. In addition, cell viability, proliferation, and morphology were affected greatly by hydrogel formulations, degradability, and cell/matrix interaction. The subtle influence of hydrogel hydrolytic degradation may be explored to enhance cell survival, proliferation, and morphogenesis (e.g., larger cell spheroids in MIN6 β cells and higher degree of cell spreading in hMSCs).

Acknowledgements: This project was funded by the NIH (R21EB013717), IUPUI Department of Biomedical Engineering (Faculty start-up fund), Office of Vice Chancellor for Research (Research Support Funds Grand), and Indiana Diabetes Research Center (Pilot & Feasibility Grant). The authors thank Dr. Chang Seok Ki and Han Shih for their technical assistance.

Received: February 4, 2013; Revised: April 9, 2013; Published online: June 17, 2013; DOI: 10.1002/mabi.201300044

Keywords: cell/material interactions; degradation; hydrogels; mesenchymal stem cells

[1] J. A. Burdick, K. S. Anseth, *Biomaterials* **2002**, *23*, 4315.
[2] J. L. Ifkovits, J. A. Burdick, *Tissue Eng.* **2007**, *13*, 2369.
[3] N. A. Peppas, J. Z. Hilt, A. Khademhosseini, R. Langer, *Adv. Mater.* **2006**, *18*, 1345.
[4] B. V. Slaughter, S. S. Khurshid, O. Z. Fisher, A. Khademhosseini, N. A. Peppas, *Adv. Mater.* **2009**, *21*, 3307.
[5] E. Jabbari, *Curr. Opin. Biotechnol.* **2011**, *22*, 655.
[6] L. M. Weber, K. N. Hayda, K. Haskins, K. S. Anseth, *Biomaterials* **2007**, *28*, 3004.
[7] J. Su, B. H. Hu, W. L. Lowe, Jr. D. B. Kaufman, P. B. Messersmith, *Biomaterials* **2010**, *31*, 308.
[8] C. C. Lin, A. T. Metters, K. S. Anseth, *Biomaterials* **2009**, *30*, 4907.
[9] D. S. Benoit, A. R. Durney, K. S. Anseth, *Biomaterials* **2007**, *28*, 66.
[10] N. S. Hwang, S. Varghese, H. Li, J. Elisseeff, *Cell Tissue Res.* **2011**, *344*, 499.
[11] S. P. Zustiak, J. B. Leach, *Biomacromolecules* **2010**, *11*, 1348.
[12] S. P. Zustiak, R. Durbal, J. B. Leach, *Acta Biomater.* **2010**, *6*, 3404.
[13] M. B. Browning, E. Cosgriff-Hernandez, *Biomacromolecules* **2012**, *13*, 779.
[14] J. S. Temenoff, H. Park, E. Jabbari, D. E. Conway, T. L. Sheffield, C. G. Ambrose, A. G. Mikos, *Biomacromolecules* **2004**, *5*, 5.
[15] J. S. Temenoff, H. Park, E. Jabbari, T. L. Sheffield, R. G. LeBaron, C. G. Ambrose, A. G. Mikos, *J. Biomed. Mater. Res., A* **2004**, *70A*, 235.
[16] H. Park, X. Guo, J. S. Temenoff, Y. Tabata, A. I. Caplan, F. K. Kasper, A. G. Mikos, *Biomacromolecules* **2009**, *10*, 541.
[17] S. J. Bryant, R. J. Bender, K. L. Durand, K. S. Anseth, *Biotechnol. Bioeng.* **2004**, *86*, 747.
[18] E. Cho, J. K. Kutty, K. Datar, J. S. Lee, N. R. Vyavahare, K. Webb, *J. Biomed. Mater. Res., A* **2009**, *90A*, 1073.
[19] S. M. Li, I. Rashkov, J. L. Espartero, N. Manolova, M. Vert, *Macromolecules* **1996**, *29*, 57.
[20] A. T. Metters, K. S. Anseth, C. N. Bowman, *Polymer* **2000**, *41*, 3993.
[21] J. W. DuBose, C. Cutshall, A. T. Metters, *J. Biomed. Mater. Res., A* **2005**, *74A*, 104.
[22] P. van de Wetering, A. T. Metters, R. G. Schoenmakers, J. A. Hubbell, *J. Controlled Release* **2005**, *102*, 619.
[23] M. P. Lutolf, J. A. Hubbell, *Nat. Biotechnol.* **2005**, *23*, 47.
[24] M. P. Lutolf, J. L. Lauer-Fields, H. G. Schmoekel, A. T. Metters, F. E. Weber, G. B. Fields, J. A. Hubbell, *Proc. Natl. Acad. Sci. USA* **2003**, *100*, 5413.
[25] J. Patterson, J. A. Hubbell, *Biomaterials* **2010**, *31*, 7836.
[26] J. J. Moon, J. E. Saik, R. A. Poche, J. E. Leslie-Barbick, S. H. Lee, A. A. Smith, M. E. Dickinson, J. L. West, *Biomaterials* **2010**, *31*, 3840.

[27] J. E. Leslie-Barbick, J. E. Saik, D. J. Gould, M. E. Dickinson, J. L. West, *Biomaterials* **2011**, *32*, 5782.
[28] B. D. Fairbanks, M. P. Schwartz, A. E. Halevi, C. R. Nuttelman, C. N. Bowman, K. S. Anseth, *Adv. Mater.* **2009**, *21*, 5005.
[29] C. C. Lin, A. Raza, H. Shih, *Biomaterials* **2011**, *32*, 9685.
[30] C. C. Lin, K. S. Anseth, *Proc. Natl. Acad. Sci. USA* **2011**, *108*, 6380.
[31] A. Raza, C. C. Lin, *J. Visualized Exp.* **2012**, *70*, e50081.
[32] H. Shih, C. C. Lin, *Biomacromolecules* **2012**, *13*, 2003.
[33] S. B. Anderson, C. C. Lin, D. V. Kuntzler, K. S. Anseth, *Biomaterials* **2011**, *32*, 3564.
[34] B. D. Fairbanks, M. P. Schwartz, C. N. Bowman, K. S. Anseth, *Biomaterials* **2009**, *30*, 6702.
[35] H. Nagase, G. B. Fields, *Biopolymers* **1996**, *40*, 399.
[36] M. P. Lutolf, J. L. Lauer-Fields, H. G. Schmoekel, A. T. Metters, F. E. Weber, G. B. Fields, J. A. Hubbell, *Proc. Natl. Acad. Sci. USA* **2003**, *100*, 5413.
[37] K. S. Anseth, A. T. Metters, S. J. Bryant, P. J. Martens, J. H. Elisseeff, C. N. Bowman, *J. Controlled Release* **2002**, *78*, 199.
[38] A. Metters, J. Hubbell, *Biomacromolecules* **2005**, *6*, 290.
[39] J. D. McCall, K. S. Anseth, *Biomacromolecules* **2012**, *13*, 2410.
[40] A. Shikanov, R. M. Smith, M. Xu, T. K. Woodruff, L. D. Shea, *Biomaterials* **2011**, *32*, 2524.
[41] M. B. Browning, T. Wilems, M. Hahn, E. Cosgriff-Hernandez, *J. Biomed. Mater. Res., A* **2011**, *98A*, 268.
[42] C. S. Bahney, T. J. Lujan, C. W. Hsu, M. Bottlang, J. L. West, B. Johnstone, *Eur. Cell Mater.* **2011**, *22*, 43.
[43] Z. G. Chang, J. M. Wei, C. F. Qin, K. Hao, X. D. Tian, K. Xie, X. H. Xie, Y. M. Yang, *Dig. Dis. Sci.* **2012**, *57*, 1181.
[44] C. S. Bahney, C. W. Hsu, J. U. Yoo, J. L. West, B. Johnstone, *FASEB J.* **2011**, *25*, 1486.
[45] K. M. Schultz, K. S. Anseth, *Soft Matter* **2013**, *9*, 1570.
[46] K. M. Schultz, A. D. Baldwin, K. L. Kiick, E. M. Furst, *ACS Macro Lett.* **2012**, *1*, 706.
[47] L. Jongpaiboonkit, W. J. King, W. L. Murphy, *Tissue Eng., A* **2009**, *15*, 343.
[48] W. J. King, L. Jongpaiboonkit, W. L. Murphy, *J. Biomed. Mater. Res., A* **2010**, *93*, 1110.
[49] G. A. Hudalla, T. S. Eng, W. L. Murphy, *Biomacromolecules* **2008**, *9*, 842.
[50] L. Jongpaiboonkit, W. J. King, W. L. Murphy, *Tissue Eng., A* **2009**, *15*, 343.
[51] W. J. King, L. Jongpaiboonkit, W. L. Murphy, *J. Biomed. Mater. Res., A* **2010**, *93A*, 1110.
[52] L. Gao, R. McBeath, C. S. Chen, *Stem Cells* **2010**, *28*, 564.